



# OPEN ACCESS INTERNATIONAL JOURNAL OF SCIENCE & ENGINEERING

## CFD ANALYSIS FOR SUPERSONIC FLOW OVER A WEDGE

<sup>1</sup> PIDATALA KIRAN KUMAR, <sup>2</sup> Smt. T. SUSEELA,

<sup>1</sup>M.Tech student, Department of Mechanical Engineering, Acharya Nagarjuna University College of Engineering and Technology, Nagarjuna Nagar, Guntur, Andhra Pradesh

<sup>2</sup>Assistant Professor, Department of Mechanical Engineering, Acharya Nagarjuna University College of Engineering and Technology, Nagarjuna Nagar, Guntur, Andhra Pradesh

<sup>1</sup> pkiran958@gmail.com, <sup>2</sup> tsuseela.anu@gmail.com

**Abstract:** A wedge is triangular shaped geometrical structure. It is mostly used as supersonic airfoils and nose of supersonic airplanes. It is typically inclined plane which is at an angle with the horizontal. This project helps in explaining most of the concepts related to wedge. In this project the principle of working of wedges with the variation of half-wedge angle and also with variation of Mach number has been done. Theoretical analysis of supersonic flow over wedge is also done. The variation of flow parameters like Pressure, Temperature and Mach number is visualised using computational fluid Dynamics and it's contours and graphs has been plotted. The simulation of shockwave (attached and detached) through CFD is also analyzed. To look at the flow qualitatively. You will solve problem in Fluent and hexa mesh in ICEMCFD. We will use online shock calculator to see Mach number after each step and as well as the flow angle.

### I INTRODUCTION

#### INTRODUCTION OF TUBULENCE

CFD based on the Reynolds Averaged Navier Stokes (RANS) equations is now widely used in the aeronautical industry during the design process. While a large number of studies are concerned with classical aerodynamic simulations at transonic speeds, an increasing number of auxiliary simulations are required to optimize the entire aircraft. This includes flows at low speeds (take-off and landing, cabin climate), multi-phase flows (icing) as well as “multi-physics” applications (fluid-structure coupling, aerodynamic noise generation, radar signature). Historically, different codes are used for the different applications. The auxiliary simulations are mostly based on general-purpose codes, while in-house or special purpose codes are used for the external aerodynamics. However, an increasing number of applications require the combination of generality with a high degree of numerical and modelling accuracy. It is therefore essential that general-purpose codes provide a level of accuracy and numerical performance satisfying the requirements of aeronautical design engineers. Aerodynamics codes are typically built on

density-based formulations, which have evolved from methods developed for the solution of the Euler equations. They are mostly optimized for tight shock resolution and nonoscillatory behavior near extrema. On the other hand, general-purpose industrial codes are generally built on pressurebased formulations like the SIMPLE or SIMPLEC schemes or more recent method like those given by Rhie and Chow .

#### 1.2 WEDGE:

A wedge is a triangular shaped or in other words a plane inclined with an angle to the horizontal

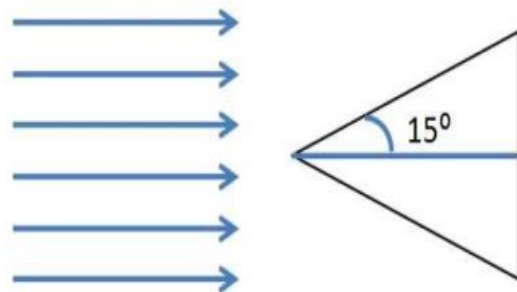


Figure 1 WEDGE

**1.3 FLOW OF A WEDGE**

As an object moves through a gas, the gas molecules are deflected around the object. If the speed of the object is much less than the speed of sound of the gas, the density of the gas remains constant and the flow of gas can be described by conserving momentum, and energy. As the speed of the object approaches the speed of sound, we must consider compressibility effects on the gas. The density of the gas varies locally as the gas is compressed by the object.

For compressible flows with little or small flow turning, the flow process is reversible and the entropy is constant. The change in flow properties are then given by the isentropic relations (isentropic means "constant entropy"). But when an object moves faster than the speed of sound, and there is an abrupt decrease in the flow area, shock waves are generated in the flow. Shock waves are very small regions in the gas where the gas properties change by a large amount. Across a shock wave, the static pressure, temperature, and gas density increases almost instantaneously. The changes in the flow properties are irreversible and the entropy of the entire system increases. Because a shock wave does no work, and there is no heat addition, the total enthalpy and the total temperature are constant. But because the flow is non-isentropic, the total pressure downstream of the shock is always less than the total pressure upstream of the shock. There is a loss of total pressure associated with a shock wave.

On this page, we consider the supersonic flow of air past a two-dimensional wedge. If the Mach number is high enough and the wedge angle is small enough, an oblique shock wave is generated by the wedge, with the origin of the shock attached to the sharp leading edge of the wedge. If we think of the oblique shock as a normal shock inclined to the flow at some shock angle  $s$ , then the normal shock relations can be applied across the shock in a direction perpendicular to the shock, and the flow component parallel to the shock remains unchanged. The resulting Mach number and speed of the flow decrease across the shock wave. For the Mach number change across an oblique shock there are two possible solutions; one supersonic and one subsonic. In nature, the supersonic ("weak shock") solution occurs most often. However, under some conditions the "strong shock", subsonic solution is possible. For a given upstream Mach number, there is a maximum wedge angle for which the shock remains attached to the leading edge. For wedge angles greater than the maximum, a detached normal shock occurs. The conditions for an attached shock is shown on the slide.

**1.4 SHOCKWAVE :** A shockwave is an extremely thin region, typically on the order of 10-5 cm across which the flow properties can change drastically.

**1.5 OBLIQUE SHOCKWAVE:** When a shockwave makes an oblique angle with respect to upstream flow, it is termed as oblique shockwave. Oblique shockwave occurs when a supersonic flow is encountered at the wedge that effectively turns the flow into itself. Oblique shock is generally created at the nose of the wedge. Downstream of the oblique shock the properties change drastically.

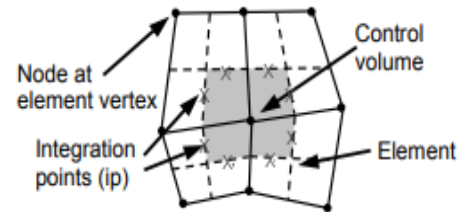


**FIGURE 2 OBLIQUE SHOCKWAVE PROPERTIES VARIATION**

**1.6 BASIC EQUATION:**

Basic equations The relevant equations of motion for aerodynamic flows are the mass, momentum and energy equations:

$$\frac{\partial \rho}{\partial t} + \frac{\partial}{\partial x_j} (\rho u_j) = 0 \tag{1}$$

$$\frac{\partial}{\partial t} (\rho u_i) + \frac{\partial}{\partial x_j} (\rho u_j u_i) = - \frac{\partial P}{\partial x_i} + \frac{\partial \tau_{ij}}{\partial x_j} + S_{u_i}$$

$$\frac{\partial}{\partial t} (\rho H - P) + \frac{\partial}{\partial x_j} (\rho u_j H) = \frac{\partial}{\partial x_j} \left( k \frac{\partial T}{\partial x_j} \right) - \frac{\partial}{\partial x_j} (u_j \tau_{ij}) + S_T$$

where  $\rho$  is density,  $u$  is velocity,  $P$  is pressure,  $\mu$  is the fluid viscosity,  $H$  is total enthalpy / 2  $H = h + u \cdot u$ ,  $h$  is the static enthalpy,  $T$  is temperature and  $\tau$  is the stress tensor. These equations are supplemented by an equation of state,  $\rho = \rho(P, T)$ , a stress-strain relation for  $\tau$  as a function of viscosity,  $\mu$ , and the strain rate, the thermal conductivity,  $k$ , and a thermodynamic enthalpy definition,  $h = h(P, T)$ . For turbulent flows, an eddy-viscosity is typically added and the equations are solved for the Reynolds averaged quantities. The general form of the equations stays the same.

**1.7 DISCRETIZATION OF THE EQUATIONS:**

The present method uses an implicit pressure-based formulation, where the primary dependent variables are  $(P, u, H)$ . This is a typical choice for general-purpose codes, as it allows an efficient treatment of incompressible flows, which are frequently encountered in industrial CFD simulations. Provisions, which have to be taken to ensure a proper coupling between the pressure and the velocity fields for flows with strong variations in density, will be described below. The control volume is constructed around an element

vertex as the dual element mesh, as shown in Figure 1. The procedure is the same for all element types (hex, tet, wedge, pyramid) The numerical accuracy of the simulation is determined by the accuracy of the representation of the surface integrals (fluxes) at the integration points in terms of the nodal variables.

**1.8 SHOCK WAVE IN AERODYNAMIC FLOWS:**

Shock wave phenomenon

Shock waves can be generally classified into four categories:

- (1) Attached shock wave, e.g. when a supersonic flow encounters an inward corner
- (2) Detached shock wave, e.g. for a supersonic flow past a blunt body
- (3) Recompression shock wave, generated to adjust to farfield pressure, e.g. for a transonic flow past the upper surface of an airfoil or for a supersonic nozzle flow with high back pressure.
- (4) Secondary induced shock wave, due to e.g. shock reflection shock-shock interaction shock-wave/boundary-layer interaction lateral jet flow interaction shows some typical examples with shock/boundary-layer interactions in the vicinity of a high-speed vehicle. Shock waves can also be generated due to explosion, combustion or lightning strike, in which local high-pressure region may appear and lead to strong shock waves moving at supersonic speed.

**1.9 TURBULENCE FLOW:**

Turbulence modeling is one of the most challenging problems in numerical flow simulation. It is common experience that different turbulence models result in different predictions, when applied to a particular complex flow. It is doubtful whether a universally valid turbulence model, capable of describing all complex flows, could be devised. Most of the turbulence models are based on the Boussinesq hypothesis, according to which the apparent turbulent shear stresses are related linearly to the rate of mean strain through an apparent scalar turbulent or “eddy” viscosity coefficient,  $\mu_t$ . However, in strongly separated flows, the actual dependence of the modeled turbulent shear stresses to the mean strain is non-linear. For alleviating this problem, various non-linear corrections have been devised. In general, non-linear models perform better than linear ones. Still, in many practical aerospace configurations, the accuracy of Reynolds Averaged Navier–Stokes (RANS) simulation results is not satisfactory. Higher order schemes, which do not require a turbulence model for closing the equations, have been developed. The present day computing power is sufficient for the application of Large Eddy Simulation (LES) to simple configurations, like those examined in the present study, although the simulated Reynolds numbers are still rather low. Guidance to

modeling of LES is provided by the more computing power demanding Direct Numerical Simulation (DNS). Nevertheless, RANS calculations will continue for many years to support the aerospace industry. Even when LES reach the level of application in aerospace components or complete configurations, it will be more economic to apply RANS in an optimization procedure and subsequently to simulate the optimum configuration by LES. Object of the present study is the turbulence modeling of flows with extensive crossflow separation, i.e., three-dimensional flows in which the separated boundary layer rolls up into longitudinal vortices. This type of separation appears in many practical aerospace configurations; for example, subsonic/supersonic flow about slender bodies or delta wings at high incidence or in components of supersonic/hypersonic air vehicles when swept shock waves interact with boundary layers

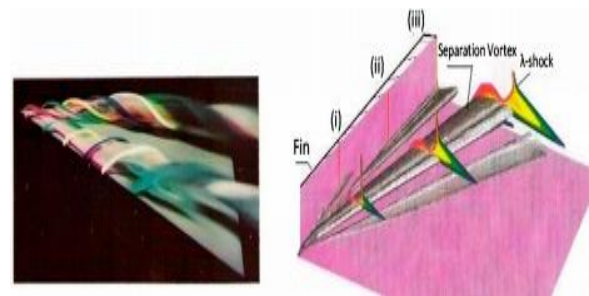


**FIGURE 3 SWEPT SHOCK/BOUNDARY LAYER INTERACTION**

**1.10 DESCRIPTION OF CODES AND TURBULENCE MODELS:**

The CFD code ISAAC, developed by Morrison [9], is used in this study. ISAAC is a second-order, upwind, finite-volume method where advection terms in the mean and turbulence equations are solved by using Roe’s approximate Riemann solver coupled with the MUSCL scheme. Viscous terms are calculated with a central difference approximation. Mean and turbulence equations are solved coupled by using an implicit spatially split, diagonalized approximate factorization solver. ISAAC has been developed to test a large range of turbulence models. Algebraic models, various  $k-\epsilon$  and  $k-\omega$  formulations, and Reynolds stress transport models are included in ISAAC. In the present article, the examined flows are calculated with the  $k-\omega$  turbulence model of Wilcox [10], the Explicit Algebraic Reynolds Stress Model (EASM) of Rumsey and Gatski [11] and a modification of the algebraic turbulence model of Baldwin and Lomax [12] done by the present author, in order to improve its accuracy in separated flows. It is known that the functional form of the Navier–Stokes equations is the same for laminar and turbulent flows. In the latter case, however, time average has been applied to equations, since in turbulent

### 1.11 HISTORY OF TURBULENCE FLOW:

In the early 1950s, H. Werle of ONERA did pioneer work in visualizing high-angle of attack flows, like the delta wing shown in Figure 1a, by using a water tunnel and injecting colors from small holes at the expected regions of generation of the separation longitudinal vortices. The appearance of separation quasi-conical vortices of flattened shape in swept shock/boundary layer interactions, like that shown in Figure 1b for a fin/plate configuration, was hypothesized in the 1970s, but it was proved much later. Indeed, this early period oil-flow visualization revealed the existence on the surface of the plate, below the separation bubble, of a separation and an attachment line, which away from the apex of the configuration are straight and intersect upstream of the apex and close to it. The trace of the inviscid shock also passes through this intersection. It has been proposed that the separation bubble is actually a conical flat vortex. More than 20 years of experimental and computational research were required for proving these early hypotheses (see [2,3] for details). Returning to turbulence modeling, it is mentioned that according to published evidence, the accuracy of prediction of flows with extensive crossflow separation is marginal. Particularly for shock wave/turbulent boundary layer interactions (SBLIs), Knight and Degrez [4] summarizing results of comparisons of several contributions (organized by Advisory Group for Aerospace Research and Development (AGARD)), using the RANS equations with a wide range of turbulence model from zero equations to full Reynolds Stress Equation formulations, state: Simulation accuracy is good for mild interactions, marginal for strong ones. For wall heat transfer rate, the deviation of the calculated results from experiment ranges from 40% to 150%. Calculations predict "more turbulent" flows, compared to experiments. To explain this condition, the present author [5] studied the effect of the longitudinal separation vortices on the turbulence of the flow. It is reminded that a characteristic feature of vortices is their strong swirling motion, allowing them to promote large-scale mixing of fluids with possibly different momentum and energy. Panaras [5] hypothesized that the longitudinal vortices generated in the types of flows shown in Figure 1, transfer external inviscid air into the lower turbulent part of the separated flow, decreasing its turbulence. To prove his hypothesis, Panaras [5] studied numerically the structure of the separation vortex, which appears in a strong swept shock wave/turbulent boundary layer interaction generated in a fin/plate configuration. He studied the flowfield by means of stream surfaces starting at the inflow plane within the undisturbed boundary layer, which is initially parallel to the plate. Each of these surfaces was represented by a number of streamlines. Calculation of the spatial evolution of selected stream surfaces revealed that the inner layers of the undisturbed boundary layer, where the eddy

viscosity is high, wind around the core of the separation vortex. However, the outer layers, which have low turbulence, rotate over the separation vortex and penetrate into the separation bubble at the attachment region, forming a low-turbulence tongue, which lies along the plate, underneath the vortex (Figure 2). The intermittency of the fluid that constitutes the tongue is very small, that is, the flow is almost laminar there. At the initial stage of development, the conical separation vortex is completely composed of turbulent fluid, but as it grows linearly downstream the low-turbulence tongue is formed. The analysis of Panaras [5] leads to the conclusion that laminarization of the initially turbulent flow appears in case of extensive crossflow separation. Hence, the Boussinesq equation is not adequate for the estimation of the Reynolds stresses. With reference to Figure 2, it is mentioned that although the mean strain is very high in the near wall reversed flow, the flow there is almost laminar. Evidently, application of Boussinesq's equation in this region predicts higher Reynolds stresses than the actual ones. Related examples will be given in Section The discovery of the laminarization of the initially turbulent flow, in flows with extensive crossflow separation led to the development of new ideas in turbulence modeling for shock wave/turbulent boundary layer interactions (SBLIs). These new ideas include realizability (weak nonlinearity) and specific physical models, which incorporate known flowfield behavior [6,7]. In a short period the simulation accuracy of SBLIs was improved. This is clearly evident if the content of the critical survey of Computational Fluid Dynamics (CFD) prediction capabilities for SBLIs prepared by Knight and Degrez [4] and of the similar review of Knight et al. [3], which was published only five years later, are compared. In spite of the spectacular improvement shown by the new models, even presently, the predicted skin friction and heat transfer are marginally accurate in simulations of flows with extensive crossflow separation. The present review has been prepared in order to stimulate further research, now that LES methods enter the field. Published and new data will be presented for 3-D SBLIs and high-alpha flows. New evidence will be given regarding the almost-laminar nature of the near wall reverse flow in these types of flow, including data from the first publication of fin/plate simulation by using

### II LITERATURE REVIEW

J. Neumann (1943) formulated the theory of two- and three-wave reflection of a shock wave from a wedge. He also expressed the idea that reflection may be right (regular) and wrong (irregular, as an alternative to the right), and Mach reflection is one of the possible types of irregular reflection. J. Neumann also qualitatively described the kind of irregular reflection, which he called nonMach and which later became known as "Neumann reflection" (Kawamura, 1956). In this

paper by W. Bleakney, C.H. Fletcher and D.K. Weimer (1949) and others the assumption of the existence of von Neumann on existence of tangential discontinuity behind the triple point was experimentally verified. In many experiments the contact discontinuity was observed, and in those cases when it is not observed, the theoretical value of the densities differential on its sides did not exceed the measurement error, and therefore it could not be detected. Thus, the model of von Neumann was proved. Following the experimental confirmation Neumann's TC model was proved theoretically. R. Courant, and K.O. Friedrichs (1948) have shown that under ideal gas model three shock waves may exist in the same point only in presence of some another surface discontinuity. In his work Courant and Friedrichs also theorized that depending on the movement direction of the triple point (T on Figure 3) the Mach reflection can be divided into three types: – Simple Mach reflection (as the shock wave propagates the triple point moves away from the wedge surface, the Mach stem increases, DiMR at Figure 3) – Stationary Mach reflection (triple point moves parallel to the surface, StMR at Figure 3) and – Reversed Mach reflection (triple point moves towards the surface, InMR at Figure 3)

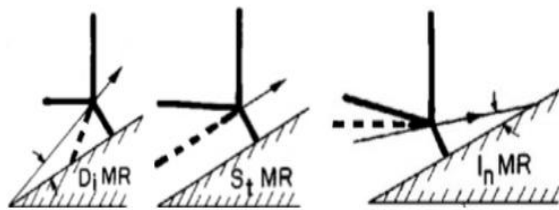


**Figure 4 Simple DiMR, stationary StMR and reversed InMR (inverse) Mach reflections of shock waves from the wedge**

In 1967 Brides developed the result of Courant and Friedrichs for the case of arbitrary equations of gas state (Breed, 1967). In 2008 V.N. Uskov together with M.V. Chernyshev (2009) presented the full research of stationary TC corresponding to von Neumann model, which was later generalized for nonstationary case (Uskov & Mostovikh, 2008). Von Neumann model for a real gas was considered by Lo for the case of oxygen (Law, 1970) for cases of nitrogen and argon. In these studies, the caloric properties of gases were described by a set of vibrational energy levels of molecules, to each of which the energy of its activation and its multiplicity was given. The work of J.-H. Lee, and I.I. Glass (1984) argues that in calculating of TC of oxygen O<sub>2</sub> and nitrogen N<sub>2</sub> it is possible to use the model of an ideal gas, and in the calculation of carbon dioxide CO<sub>2</sub> and sulfur hexafluoride SF<sub>6</sub> it is required to use a model of imperfect gas. Comparison of different models of diatomic non-perfect gas in the annex to TC calculation was performed by V.N. Uskov and P.S. Mostovikh (2011). Purpose of the work is to

show how the phenomena of Mach reflection of shock waves from the wedge was being studied on an example of the most significant scientific works. Irregular (Mach) reflection of gas-dynamic discontinuities (GDD) from obstacle is discussed. The researches of Mach and von Neumann, which created the foundation for the study of different types of shock waves triple configurations are presented. The history of studying triple configurations arising in supersonic jets is presented as well. Article also discusses the main types of Mach reflection and their classification.

A detailed overview of the state of this question is given in W. Bleakney, and A.H. Taub (1949). As the authors note, there is poor compliance of the experimental results with the predictions of von Neumann theory for small wedge angles and in area of parameter values close to the transition from regular reflection to Mach reflection. The disagreement between the experimental data and the theory predictions, according to the review, cannot be explained by the wrongness of von Neumann's assumptions about the structure of TC. Experimental studies and theoretical method of analyzing the shock polars, proposed in 1956, by R. Kawamura, and H. Saito (1956) also gave no satisfactory agreement between theory and experiment. W. Bleakney and A.H. Taub (1949) in the aforementioned review article, on the basis of experimental results obtained by them and on Smith's experimental data, and have plotted the wedge angle at which the transition of an incident shock wave to a Mach reflection occurs, by its intensity. According to them, the transition occurs in an area where regular reflection is theoretically impossible (required rotation angle of the flow is greater than the critical rotation angle on the shock wave). This criterion is called the criterion of disconnection (of the shock polar from ordinate axis) or von Neumann criterion. Smith's results were experimentally confirmed by Kawamura and Saito. It was also found that with increase of shock wave intensity the region of small angles at wedge's apex, for which the von Neumann theory is distant from the experiment, is reduced. In contrast, the range of angles at which the transition from regular reflection to Mach reflection occurs and both types of reflection are theoretically possible increases. Paying attention to the fact that in a certain range of wedge angles the shock polar axis intersects both the ordinate and the upper branch of isomach, i.e. both regular and Mach reflection are theoretically possible, Neumann suggested another criterion of transition from regular reflection to Mach reflection, somewhat poorly calling it "the criterion of mechanical equilibrium." According to this criterion, the transition should occur at the moment when a shock polar crosses with an isomach at its peak, i.e., the intensity of the Mach stem in this case is equal to maximum for a given Mach number, which determines an isomach (Figure 5). SWS, which occurs at this

is moment called a stationary Mach configuration (StMC). That is why this criterion was named “StMC criterion” by V. N. Uskov. On the figure 5:  $\beta_1$  - flow rotation angle on the incoming shock,  $\beta_2$  - flow rotation angle on the reflected shock,  $\Lambda_1$  logarithm of incoming shock’s intensity,  $\Lambda_2$  logarithm of reflected shock’s intensity,  $\Lambda_3$  logarithm of Mach stem intensity. Subsequent studies have shown that a hysteresis often occurs, i.e. with increase of the angle the transition from regular to irregular reflection occurs at intensity close to the criterion of disconnection, and with a decrease of the shock’s incline angle the reversed transition is closer to the StMC criterion. A lot of papers are dedicated to this issue. In 70s – 80s of 20-th century the search for other criteria and/or the confirmation of von Neumann criterion was the subject of numerous experimental researches conducted in shock tubes. During the experiments, the disconnection criterion was confirmed by Henderson and Lozzi for steady flows of diatomic gases at oncoming wave’s Mach numbers from 1 to 4, by Hornung and Kichakoff for argon at incident shock wave’s Mach number up to 16, for pseudo-stationary cases – by Hornung, Oertel and Sandeman, for pseudostationary flows, simple, complex and double Mach reflection – in the works of G. Ben-Dor, and I.I. Glass (1980). Guderley’s 3 – waves model for Mach reflection of a weak shock waves and other models. In addition to von Neumann model, several other possible local patterns of the flow at the triple point of Mach reflection were suggested. In 1959, Sternberg suggested that in the immediate vicinity of the triple point the tangential discontinuity surface is not fully formed. Sternberg calculated the flow in the vicinity of TC triple point taking into account the gas viscosity. Description of the triple point without using the SWS on GDD, i.e. without using the Rankin-Hugoniot relations was first undertaken in 1964 in the work of A. Sakurai (1964). He received an approximate analytical solution of NavierStokes equations in vicinity of triple point. A. Sakurai (1964) found gas-dynamic parameters in the vicinity of triple point depending on the polar angle and showed that at very low shock intensity his theory corresponds better to the experiment than von Neumann theory. At high shock intensities, on the contrary, von Neumann theory is more accurate. This result appears to be natural. In a close vicinity of interference point the influence of real gas properties is strong, and the shock waves cannot be considered infinitely thin. With the increase of distance from the point of interference the accuracy of equations’ factorization in a row of by small parameter decreases. It is worth to mention the very exotic hypotheses as. In the paper by V.G. Dulov (1973), it was suggested that it is not one, but two tangential discontinuity coming out from the triple point, however, this assumption didn’t found experimental confirmation and didn’t get the mathematical development. At present, the von

Neumann model is considered generally recognized. Nevertheless, an unexplained Neumann paradox remains (Bleakney, Fletcher & Weimer, 1949). Recall that for Mach numbers less than a special number of

$$M_T = \sqrt{\frac{2-\varepsilon}{1-\varepsilon}}, \quad \varepsilon = \frac{\gamma-1}{\gamma+1},$$

the solution for irregular reflection of the shock wave from the wall with forming of a triple point is absent. However, it is observed experimentally,  $\gamma$ adiabatic parameter equal to the ratio between the heat capacity at constant pressure and the heat capacity at constant volume. For nearly forty years the experiments were conducted, sometimes being very subtle, which clearly demonstrated that the three-wave theory does not work for the reflection of weak shock waves with Mach number of incident flow less than  $M_t$ . For weak shock waves (small Mach numbers) Guderley suggested a fourwave model (Figure 6) with an additional rarefaction wave behind the reflected discontinuity. A similar pattern was researched in the work of E.I. Vasilev, and A.N. Kraiko (1999). For a long time, it was not possible to obtain a numerical solution for this kind of flows as well, until E. I. Vasilev (1999) has shown that the problem lies in the lack of accuracy of numerical methods, the influence of "circuit" computing viscosity and parasitic oscillations of the solution, and the flow corresponds to Guderley’s "four-wave" model. For this end, a numerical method with the highlight of discontinuities was used. Finally, V.N. Uskov constructed a harmonious classification of the interference of stationary gasdynamic discontinuities which showed that triple configurations are of three types, and the Guderley model is just a special case of interference of overtaking shocks. In addition, generally speaking, it is not quite correct, because shock wave called Guderley reflected (RS in Figure 6), is actually a second coming shock wave.

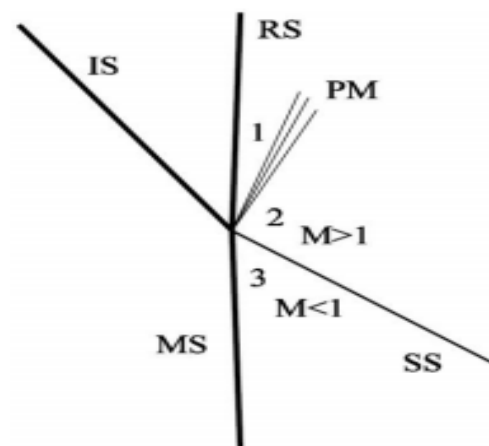
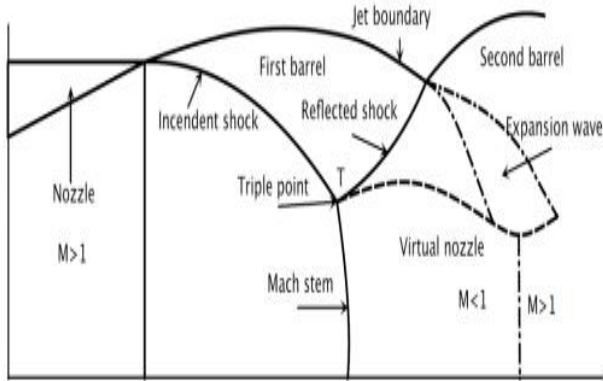


Figure 5 Configuration of SWS



**Figure 6 Explanation to Abbet procedure of finding Mach disk position in supersonic axisymmetric jet**

Considering this flow one-dimensional, it is possible to perform the analysis in the same way as in the Laval nozzle. If the result in minimum section of flow behind the Mach disk speed is equal to the local sonic speed, then in Abbet-Dash procedure it is considered that the location of Mach disk in the jet is selected correctly. Continuing development of this model S.M. Dash has shown that it is close to the experimental results only in certain flow regimes and it is easier to calculate the Mach disk using implicit methods for solution of parabolic NavierStokes equations (Dash & Roger, 1981). Among other models well-confirmed is the criterion according to which the formation of Mach disc occurs when the intensity of the incident shock reaches  $J = J_0$ , corresponding to stationary Mach configuration. In StMC (Figure 5) the main shock wave is straightforward. The characteristic intensity  $J_0$  is obtained by solving the cubic equation, corresponding to the polars' intersection at the top of main polar.

$$\begin{aligned}
 A_3 &= 1 - \varepsilon^2, \\
 A_2 &= -\left((1 + \varepsilon - \varepsilon^2 + \varepsilon^3)J_m + 1 + \varepsilon^2\right), \\
 \sum_{k=0}^3 A_k J_0^k &= 0, \quad A_1 = \varepsilon(1 + J_m)[(1 - \varepsilon)J_m - 2], \\
 A_0 &= (1 - \varepsilon)J_m(J_m - 1), \\
 J_m &= (1 + \varepsilon)M^2 - \varepsilon.
 \end{aligned}$$

Indirect justification for  $J_0$  criterion is the solution of the first order problem on shock waves (shocks) triple configurations, obtained by V.N. Uskov (2012) still in his doctoral study and published in 2012 (Uskov, Bulat & Prodan, 2012). Its essence lies in the fact that if at each point of suspended (falling on the axis of symmetry) shock a formal calculation of triple shock wave configuration (Figure 8) would be done, then with intensities  $J < J_0$  triple configuration belongs to TC-1 type and the outgoing tangential discontinuity  $\tau$  has a positive curvature (1 and 2 in Figure 8). At the point of shock, where  $J$

=  $J_0$  (StMR), the curvature  $\tau$  becomes negative, which corresponds to the prevailing of empirical understanding of tangential discontinuity form

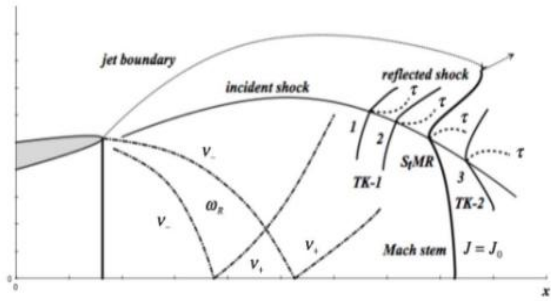


**Figure 7 On the justification of stationary Mach configuration model for Mach disc in supersonic under expanded jet**

Triple configuration corresponds to the transition type TC-1/2 (StMCSMR). When the triple point is located down the stream (point 3 in Figure 8) triple configuration would belong to the type TC-2. Stationarity criterion of Mach configuration was strictly proved by P.V. Bulat in 2012 (Uskov, Bulat & Prodan, 2012), using the theory of features of smooth reflections, developed for shock waves under the leadership of V.I. Arnold. Comparison of calculation results with experimental results showed a good agreement. In the work a method for estimating the size of Mach shock in overexpanded jet is developed, with the dependence of its size on the pressure ratio being nonisobaric and becoming zero at the parameters of the jet corresponding the von Neumann criterion. Thus, the question of the criteria for transition to Mach reflection in the axially symmetric case can be considered closed. Transition occurs when the incident shock wave reaches the intensity of  $J_0$ , appropriate to StMC

### III PROJECT OVER VIEW

#### 3.1 OBJECTIVE OF THE PROJECT:

1. To look at the flow qualitatively. You will solve problem in Fluent and hexa mesh in ICEMCFD.
2. We will use online shock calculator to see Mach number after each step and as well as the flow angle.
3. Hexa mesh was made in ICEMCFD
4. Total number of nodes = 1.37 million
5. Choosing turbulence flow in inviscid
6. Finally find out the discuss about the Mach no and angle of shock at each step of Wedge

#### 3.2 METHODOLOGY:

1. This is triple wedge with flow coming at Mach No. = 3. Thickness of wedge = 0.5 m
2. Inlet static pressure = 101325 Pa and inlet static temp = 288 K
3. Operating pressure = 0 Pa.

4. Flow is assumed to be compressible (ideal gas) and is solved as inviscid flow. You can run it as viscous flow (i.e. running with turbulence model such as SA or SST models).
5. Geometry file is provided as .tin file along with domain.

**3.3 DIMENSIONS OF THE TRIPLE WEDGE:**

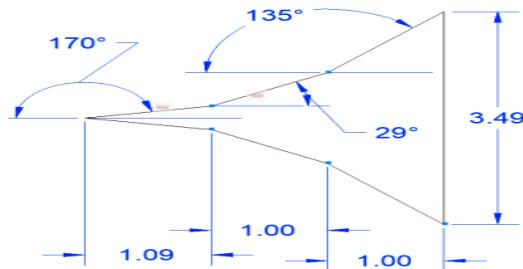


**Figure 8 On the justification of stationary Mach configuration model for Mach disc in supersonic under expanded jet**

**IV INTRODUCTION OF ANSYS**

ANSYS is a large-scale multipurpose finite element program developed and maintained by ANSYS Inc. to analyze a wide spectrum of problems encountered in engineering mechanics.

**V COMPUTATIONAL FLUID DYNAMICS**

**5.1 INTRODUCTION OF CFD:**

Computational Fluid Dynamics (CFD) is a computer-based tool for simulating the behavior of systems involving fluid flow, heat transfer, and other related physical processes. It works by solving the equations of fluid flow (in a special form) over a region of interest, with specified (known) conditions on the boundary of that region.

**5.2 THE HISTORY OF CFD :**

Computers have been used to solve fluid flow problems for many years. Numerous programs have been written to solve either specific problems, or specific classes of problems. From the mid-1970s, the complex mathematics required to generalize the algorithms began to be understood, and general purpose CFD solvers were developed. These began to appear in the early 1980s and required what were then very powerful computers, as well as an in-depth knowledge of fluid dynamics, and large amounts of time to set up simulations. Consequently, CFD was a tool used almost exclusively in research. Recent advances in computing power, together with powerful graphics and interactive 3D manipulation of models, have made the process of creating a CFD model and analyzing results much less labor intensive, reducing time and, hence, cost. Advanced solvers contain algorithms that enable robust solutions of the flow field in a reasonable time. As a result of these factors, Computational Fluid Dynamics is now an established industrial design tool, helping to reduce

design time scales and improve processes throughout the engineering world. CFD provides a cost-effective and accurate alternative to scale model testing, with variations on the simulation being performed quickly, offering obvious advantages.

The Mathematics of CFD The set of equations that describe the processes of momentum, heat and mass transfer are known as the Navier-Stokes equations. These partial differential equations were derived in the early nineteenth century and have no known general analytical solution but can be discretized and solved numerically. Equations describing other processes, such as combustion, can also be solved in conjunction with the Navier-Stokes equations. Often, an approximating model is used to derive these additional equations, turbulence models being a particularly important example. There are a number of different solution methods that are used in CFD codes. The most common, and the one on which CFX is based, is known as the finite volume technique. In this technique, the region of interest is divided into small sub-regions, called control volumes. The equations are discretized and solved iteratively for each control volume. As a result, an approximation of the value of each variable at specific points throughout the domain can be obtained. In this way, one derives a full picture of the behavior of the flow.

**5.3 USES OF CFD**

CFD is used by engineers and scientists in a wide range of fields. Typical applications include:

- Process industry: Mixing vessels, chemical reactors
- Building services: Ventilation of buildings, such as atriums
- Health and safety: Investigating the effects of fire and smoke
- Motor industry: Combustion modeling, car aerodynamics
- Electronics: Heat transfer within and around circuit boards
- Environmental: Dispersion of pollutants in air or water
- Power and energy: Optimization of combustion processes
- Medical: Blood flow through grafted blood vessels

**VI CFX**

**6.1 INTRODUCTION OF CFX:**

ANSYS CFX is a general purpose Computational Fluid Dynamics (CFD) software suite that combines an advanced solver with powerful pre- and post-processing capabilities. It includes the following features:

- An advanced coupled solver that is both reliable and robust.
- Full integration of problem definition, analysis, and results presentation.
- An intuitive and interactive setup process, using menus and advanced graphics.

ANSYS CFX is capable of modeling:

- Steady-state and transient flows
- Laminar and turbulent flows
- Subsonic, transonic and supersonic flows
- Heat transfer and thermal radiation
- Buoyancy
- Non-Newtonian flows
- Transport of non-reacting scalar components
- Multiphase flows
- Combustion
- Flows in multiple frames of reference
- Particle tracking.

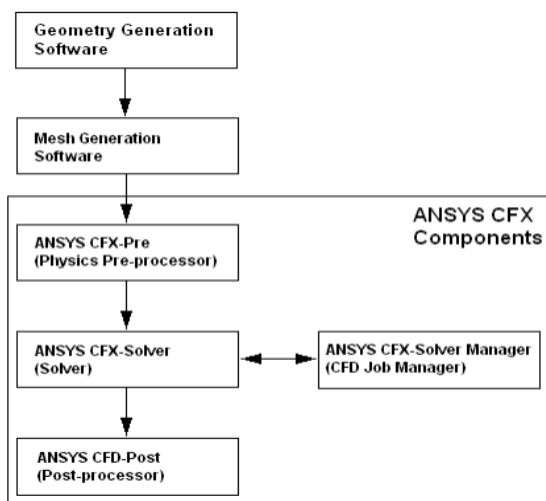


Figure 9 show the file types involved in this data flow

### 6.2 CFX-PRE-PROCESSOR:

The next-generation physics pre-processor, CFX-Pre, is used to define simulations. Multiple meshes may be imported, allowing each section of complex geometries to use the most appropriate mesh. Analyses, which consist of flow physics, boundary conditions, initial values, and solver parameters, are also specified. A full range of boundary conditions, including inlets, outlets and openings, together with boundary conditions for heat transfer models and periodicity, are all available in ANSYS CFX through CFX-Pre; for details, see CFX-Pre Basics in the CFX-Pre User's Guide. Complex simulations are assembled from one or more configurations, each of which combines an analysis definition with other related tasks such as remeshing. Control over the configuration execution order and inter-configuration solution dependencies then facilitates the setup of relatively common simulations, such as those involving the initialization of a transient analysis using results from a steady-state analysis. Use of multiple configurations and control also facilitates the setup of increasingly complex

simulations of, for example, performance curves for turbo-machines or internal combustion engines with evolving geometry and physics.

### 6.3 CFX-Solver

CFX-Solver solves all the solution variables for the simulation for the problem specification generated in CFX-Pre.

One of the most important features of ANSYS CFX is its use of a coupled solver, in which all the hydrodynamic equations are solved as a single system. The coupled solver is faster than the traditional segregated solver and fewer iterations are required to obtain a converged flow solution.

### 6.4 CFX-SOLVER MANAGER :

The CFX-Solver Manager module provides greater control to the management of the CFD task. Its major functions are:

- Specify the input files to the CFX-Solver.
- Start/stop the CFX-Solver.
- Monitor the progress of the solution.
- Set up the CFX-Solver for a parallel calculation

### 6.5 CFD-POST:

CFD-Post provides state-of-the-art interactive post-processing graphics tools to analyze and present the ANSYS CFX simulation results. Important features include:

- Quantitative post-processing
- Report generation (see Report in the CFD-Post User's Guide)
- Command line, session file, or state file input (see File Types Used and Produced by CFD-Post in the CFD-Post User's Guide)
- User-defined variables
- Generation of a variety of graphical objects where visibility, transparency, color, and line/face rendering can be controlled (see CFD-Post Insert Menu in the CFD-Post User's Guide)
- Power Syntax to allow fully programmable session files (see Power Syntax in ANSYS CFX in the CFX Reference Guide). Additional information on CFD-Post is available; for details, see Overview of CFD-Post

## VII INTRODUCTION OF FEA:

The Basic concept in FEA is that the body or structure may be divided into smaller elements of finite dimensions called "Finite Elements". The original body or the structure is then considered as an assemblage of these elements connected at a finite number of joints called "Nodes" or "Nodal Points". Simple functions are chosen to approximate the displacements over each finite element. Such assumed functions are called "shape functions". This will

represent the displacement with in the element in terms of the displacement at the nodes of the element.

The Finite Element Method is a mathematical tool for solving ordinary and partial differential equations. Because it is a numerical tool, it has the ability to solve the complex problems that can be represented in differential equations form. The applications of FEM are limitless as regards the solution of practical design problems.

Due to high cost of computing power of years gone by, FEA has a history of being used to solve complex and cost critical problems. Classical methods alone usually cannot provide adequate information to determine the safe working limits of a major civil engineering construction or an automobile or an aircraft. In the recent years, FEA has been universally used to solve structural engineering problems. The departments, which are heavily relied on this technology, are the automotive and aerospace industry. Due to the need to meet the extreme demands for faster, stronger, efficient and lightweight automobiles and aircraft, manufacturers have to rely on this technique to stay competitive.

**MESHING AND BOUNDARY CONDITIONS:**

To look at the flow qualitatively. You will solve problem in Fluent and hexa mesh in ICEMCFD. We will use online shock calculator to see Mach number after each step and as well as the flow angle

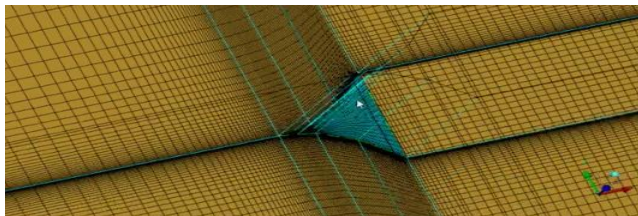


**FIGURE 3 HEXAMESH IN ICEMCFD**

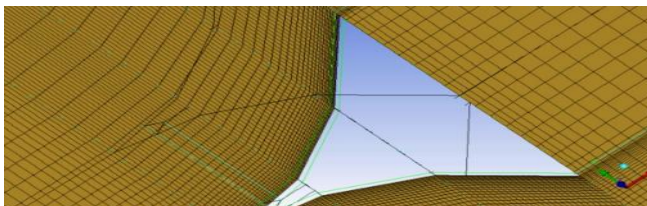


**FIGURE 4 HEXAMESH WIREFRAME OF WEDGE**

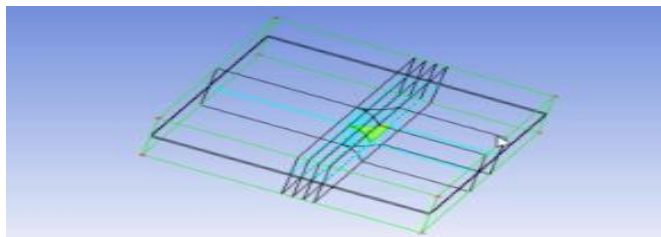


**Figure 5 Wireframe view of hexamesh wedge with boundary**

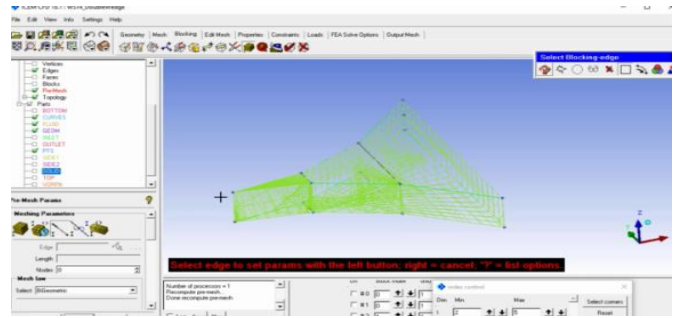


**Figure 6 Wedge in wire frame**

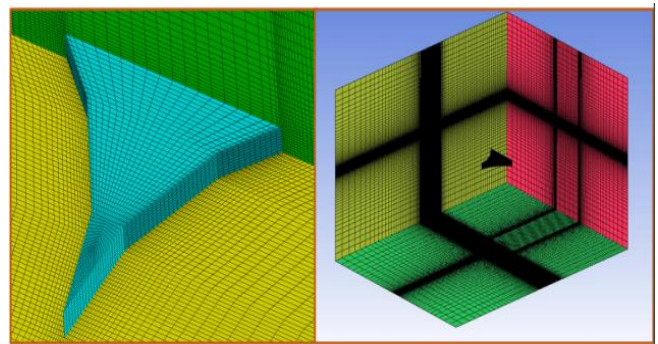


**Figure 7 Hexa mesh was made in ICEMCFD**

**VIII PROBLEM SOLVING IN SOLVENT:**

The next step is solver. In solver the solution is initialized and calculation is preceded with the desired number of iterations. It is the most important step of CFD analysis. Using Ansys-Fluent, it is possible to solve the governing equation related to the flow physical properties. Taking boundary conditions is Static pressure is 101325 pa on inlet and Mach No=3 in this project consider the Turbulence model in inviscid and chossing solution methods is implicit and flux type Run calculation is select the supersonic flow type and courant number is 0.1 and it can increase up to 120 .

Boundary Conditions	Mach = 3, static pressure = 101325 Pa on inlet
Turbulence model	Inviscid
Solution methods	Implicit, Flux type = AUSM, Flow scheme = 2 <sup>nd</sup> order upwind
Solution initialization	From inlet
Run Calculation	<ol style="list-style-type: none"> <li>1. Solution steering with supersonic flow type.</li> <li>2. Courant number = 0.1 and it can increase up to 120.</li> <li>3. Flow scheme is 0% (first to higher order blending) for first few iterations and then gradually increased up to 80%.</li> <li>4. Run calculation for 1000 – 100000 iterations depdeing on the residual plots.</li> </ol>

**FIGURE 8 BOUNDARY CONDITIONS**

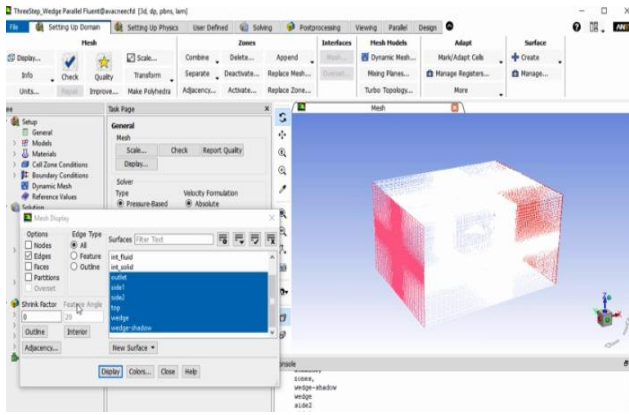


FIGURE 16 SOLVE PROBLEM IN FLUENT

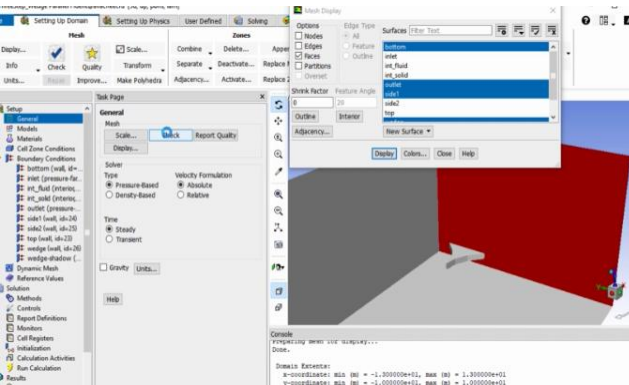


FIGURE 17 SELECT THE BOUNDARY

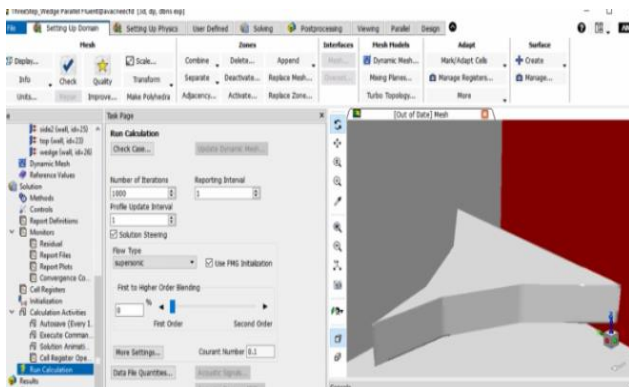


FIGURE 18 APPLY THE SUPER SONIC FLOW

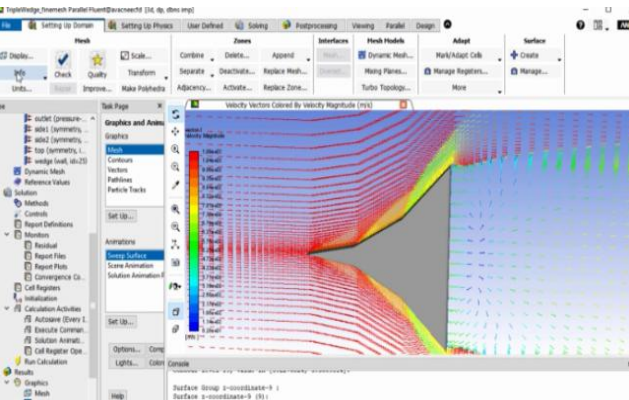


FIGURE 19 VELOCITY VECTORS PLOT

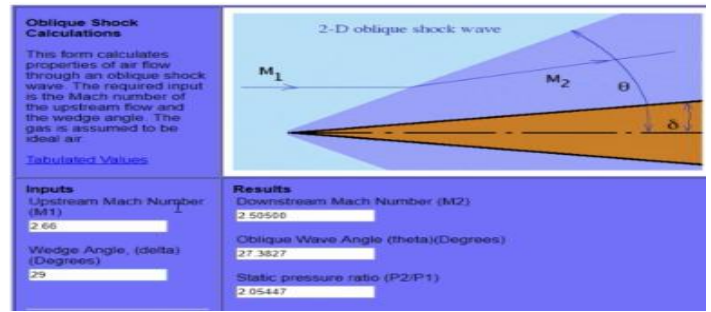


FIGURE 20 OBLIQUE SHOCK CALCULATIONS

IX RESULTS AND DISCUSSION

Design and Analysis is done in Ansys software In this project triple wedge with flow coming at Mach No. = 3. Thickness of wedge = 0.5 m .Inlet static pressure = 101325 Pa and inlet static temp = 288 K .Operating pressure = 0 Pa. Flow is assumed to be compressible (ideal gas) and is solved as inviscid flow. You can run it as viscous flow (i.e. running with turbulence model such as SA or SST models). Geometry file is provided as .tin file along with domain as shown below figures.

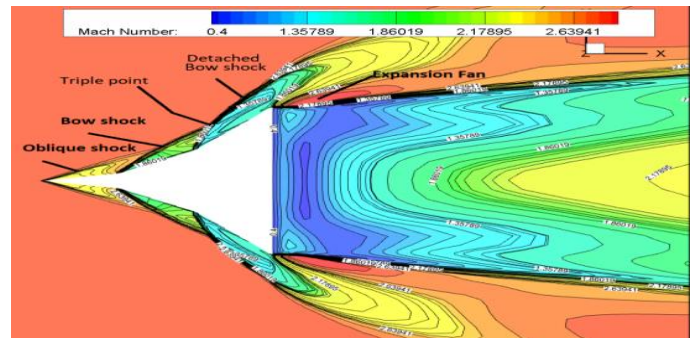


FIGURE 21 TRIPLE POINT WEDGE X CONCLUSION

The results from  $\theta$ - $\beta$ -M relation are analyzed with the help of CFD. By this Project we have explained the basic concepts connected with wedges. The study of attached and detached shockwave has been done. The effect of increasing upstream Mach number at constant wedge angle and also the effect of increasing wedge angle at constant upstream Mach number has been analyzed through CFD. We will use online shock calculator to see Mach number after each step and as well as the flow angle. You will solve problem in Fluent and hexa mesh in ICEMCFD Through this study and analysis, we have found out the values of variation of parameters such as pressure, density, temperature and Mach number by theoretical method and also using CFD. Thus we can conclude that values of these methods are approximately similar to each other. We should expect to get the flow features as shown in following two pictures.

## REFERENCES

- [1]. John D Anderson Jr, 2010 Fundamentals of Aerodynamics, 5 Edition.
- [2]. Ramesh Kolluru and Vijay Gopal 2012 Proc. Excerpt Comsol p 1.
- [3]. Pritam Kumar Patel and M Premchand CD adapco, CFD basics, American Agency, Training Document, P 38.
- [4]. Colleen D. Scott-Pomerantz 2004 The k-epsilon model in the theory of turbulence. Tech. Rep. Univ. of Pittsburgh. P 10.
- [5]. Ben-Dor, G. & Glass, I. I. (1980) Domains and boundaries of non-stationary oblique shock-wave reflexions. 2. Monatomic gas. Journal of Fluid Mechanics, 96(4), 735-756.
- [6] Bleakney, W., Fletcher, C. H. & Weimer, D. K. (1949) The density field in mach reflection of shock waves. Physical Review, 76, 323-324.
- [7] Bleakney, W. & Taub, A. H. (1949) Interaction of shock waves. Review of Modern Physics, 21, 584.
- [8] Breed, B. R. (1967) Impossibility of three confluent shocks in two-dimensional irrotational flow. Physics of Fluids, 10(1), 21-23.
- [9] Brown, G. L. & Roshko, A. (1974) On density effects and large structure in turbulent mixing layers. Journal of Fluid Mechanics, 64(4), 775-816.
- [10] Courant, R. & Friedrichs, K. O. (1948) Supersonic flow and shock waves. New York: Interscience, 464 p
- [11] Dash, S. M. & Roger, D. T. (1981) Shock-Capturing model for one- and two-phase supersonic exhaust flow. AIAA Journal, 19(7), 842-851.
- [12] Dulov, V. G. (1973) Motion of triple configuration of shock waves with formation of wake behind branching point. Journal of Applied Mechanics and Technical Physics, 14(6), 791-797. [13] Kawamura, R. & Saito, H. (1956) Reflection of Shock Waves-I Pseudo-Stationary Case. Journal of the Physical Society of Japan, 11(5), 584-592.
- [14] Landau, L. D. & Lifshitz, E. M. (2003) Theoretical Physics. London: Publishing house "Fizmatlit". 257p.
- [15] Law, C. K. (1970) Diffraction of strong shock waves by a sharp compressive corner. Toronto: University of Toronto Institute for Aerospace. 150p. Lee, J. H. & Glass, I. I. (1984) Pseudo-stationary oblique-shock-wave reflections in frozen and equilibrium air. Progress in Aerospace Sciences, 21, 33-80.
- [16] Mach, E. Uber den Verlauf von Funkenwellen in der Ebene und im Raume. Sitzungsbr Akad Wien, 78, 819-838.
- [17] Melnikov, D. A. (1962) Reflection of shock waves from the axis of symmetry. Journal of USSR Academy of Science. Mechanics and Mechanical Engineering, 3, 24-30.
- [18] Neumann, J. (1943) Oblique reflection of shocks. In A.H. Taub (ed.) John von Neumann Collected Works, 4, 238-299.
- [19] Ragab, S. A. & Wu, J. L. (1989) Linear instabilities in two-dimensional compressible mixing layers. Physics of Fluids A: Fluid Dynamics, 1(6), 957-966.
- [20] Sakurai, A. (1964) On the problem of weak mach reflection. Journal of the Physical of Japan, 19(8), 1440-1450. Smith, L. G. (1945) Photographic investigations of the reflection of plane shocks in air. Office of Scientific Research and Development, Report, 6271.
- [21] Sternberg, J. (1959) Triple-Shock-Wave Intersections. Physics of Fluids, 2(2), 179-206. 1162 P. V. BULAT Uskov, V. N., Bulat, P. V. & Prodan, N. V. (2012) Rationale for the use of models of stationary mach configuration calculation of mach disk in a supersonic jet.